Large matrix polymer solar cells fabricated by low cost air-brush spray deposition*

CHEN Zheng (陈征)[1,2], **DENG Zhen-bo** (邓振波)[2]**, **LÜ Zhao-yue** (吕昭月)[3], **ZHOU Mao-yang** (周茂杨)[2], **ZHU Li-jie** (朱丽杰)[2], **YIN Yue-hong** (殷月红)[2], **and LI Xiong** (李熊)[2]

1. *National Teaching Center for Experimental Physics, Department of Physics, School of Science, Beijing Jiaotong University, Beijing 100044, China*
2. *Key Laboratory of Luminescence and Optical Information, Ministry of Education, Institute of Optoelectronic Technology, Beijing Jiaotong University, Beijing 100044, China*
3. *Department of Physics, School of Science, East China University of Science and Technology, Shanghai 200237, China*

(Received 10 April 2015)

In this paper, a 64 mm×64 mm matrix polymer solar cell (PSC) was fabricated by air-brush spray deposition. Although the open-circuit voltage (V_{oc}) and the fill factor (*FF*) both need to be improved, the efficiency of matrix PSCs still reaches about 1.82%, and especially the current density achieves nearly 20 mA/cm^2. The results verify that air-brush spray deposition is a suitable method to prepare large area PSC devices, and the process we use in this paper can be easily transplanted to roll-to-roll production.

Document code: A **Article ID:** 1673-1905(2015)04-0244-4
DOI 10.1007/s11801-015-5058-2

Polymer solar cells (PSCs) have attracted great attention because of their several advantages, such as flexibility, light weight and controllable energy level of materials[1-5]. In recent years, remarkable progress has been made in this feild. The reported highest conversion efficiency in laboratory has achieved 9%[6,7]. It seems that PSCs could be commercialized in the near future. But so far, most of works on PSCs are focused on new materials synthesis and new device structures design, and most of devices are fabricated by spin coating.

Spin coating is very successful in laboratory. However, it doesn't work for large and flexible devices[8]. Developing a fast, large-area compatible and low-cost PSC fabrication method is an inevitable task before industrial production. Scientists have already put forword ink-jet[9,10], screen printing[11] and spray deposition[12] methods. Air-brush spray deposition is quite simple, which is widely used for painting in commercial production and suitable for industrial roll-to-roll process. Researchers have already confirmed that the performance of small size PSCs fabricated by air-brush spray deposition can be compared with that of PSCs fabricated by spin coating[12,13]. In this paper, a large (64 mm×64 mm) matrix PSC device is fabricated by scanning air-brush nozzle on the indium-tin-oxide (ITO) substrate. The research results prove that the air-brush spray deposition is suitable for not only the small size PSC devices but also the large area devices, and it has great potential for industrial production.

The schematic diagram of air-brush system is shown in Fig.1(a), the scan path of nozzle is shown in Fig.1(b), and the device structure is shown in Fig.1(c).

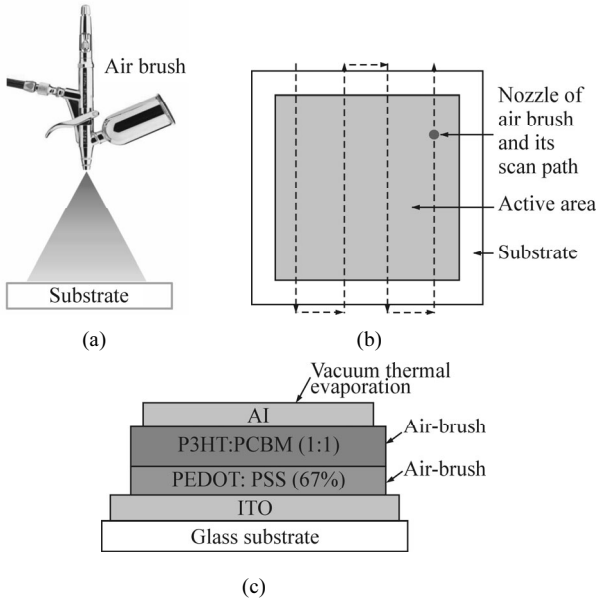

Fig.1 Schematic diagrams of (a) air-brush system, (b) scan path of nozzle and (c) PSC device structure

* This work has been supported by the National Natural Science Foundation of China (No.61274063).
** E-mail: zbdeng@bjtu.edu.cn

In the device fabrication process, a 150 nm-thick ITO layer was deposited on a cleaned glass substrate. The buffer layer and the active layer were prepared by air-brushing (IWATA-HP) poly (3,4-ethylene-dioxythiophene): poly(styrenesulfonate) (PEDOT:PSS) water solution with volume concentration of 66.7%, poly-(3-hexylthiophene) (P3HT): [6,6]-phenyl-C61-butyric-acid-methyl-ester (PCBM) chlorobenzene solution with mass ratio of 1:1 and total mass concentration of 10 mg/mL on cleaned ITO substrates, respectively, under a scan mode. During the air-brush spray deposition process, the substrate was held on hot plate, then scanned over by the air brush nozzle. The scan path is snakelike as shown in Fig.1(b). To ensure the thickness of polymer layer in active area is uniform, the scan path is beyond active area while nozzle is moving horizontally. This path is equivalent to the situation of roll-to-roll process, where the air-brush nozzle only moves in vertical direction and substrate moves in horizontal direction. After air brushing, aluminum (Al) cathode was fabricated by heat evaporation in vacuum chamber. There were two annealing processes both at 130 °C for 20 min during the preparation, which were done before and after Al cathode evaporation, respectively. The details of air-brushing process are shown in Tab.1. In addition, ITO anode on the substrate was patterned into 256 horizontal stripes with width of 0.12 mm and gap of 0.13 mm by lithography. Al cathode of device was also patterned into 64 vertical stripes with width of 0.9 mm and gap of 0.1 mm by mask. The microscope photographs of both anode and cathode are shown in Fig.2. Therefore, the finished matrix device consists of 16 384 small PSCs with scale of 0.12 mm×0.9 mm.

Tab.1 Preparation conditions of PSC device by air-brush spray deposition

Layer	Carrier gas	Pressure	Temperature of substrate	Distance from nozzle to substrate	Amount of solution
Buffer layer (PEDOT:PSS)	Dry nitrogen	~0.5 MPa	80 °C	~30 cm	3 mL
Active layer (P3HT:PCBM)	Dry nitrogen	~0.5 MPa	120 °C	~20 cm	5 mL

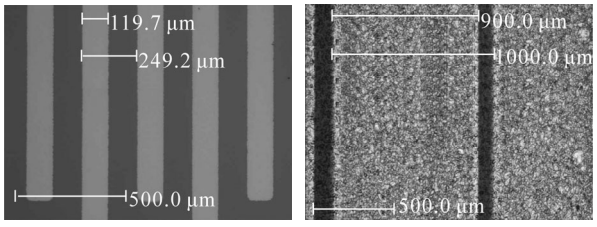

(a) (b)

Fig.2 Microscope photographs of (a) ITO anode and (b) Al cathode

The microscope photograph of the final matrix device was taken by LEICA-DMRX, the surface profile and thickness of polymer film were measured by XP-II profile meter, the current density-voltage (*J-V*) curves of device with and without annealing were measured by Keithley 2410 under a standard solar simulator at 100 mW/cm^2 with AM1.5 filter, and the incident photon-to-current conversion efficiency (IPCE) spectrum of the device was measured by Zolix Solar Cell Scan 100. It is hard to measure the whole matrix at once because of the hardware limitation. Thus several small PSCs located in different regions were selected as representatives. All these measurements were done at atmospheric environment under room temperature.

The photogragh of matrix PSC device is shown in Fig.3(a), and the microscope photograph of the device without cathode is shown in Fig.3(b). A lot of spots can be found in the microscope photograph. The scale of these spots is dozens of microns, which is mainly decided by

$$D_{\text{spots}} = k \cdot W_{\text{break}} \frac{\sigma_{\text{Solution}} \rho_{\text{Gas}}}{\mu^2 \rho_{\text{Solution}} \Delta P}, \tag{1}$$

where D_{sports} is the diameter of spots, k is the ratio between spot diameter and the scale of atomized droplets, W_{break} is an characteristic factor, which is defined to describe the critical condition of atomizing process, σ_{Solution} is the surface tension of the solution, ρ_{Gas} is the density of carrier gas, μ is the flow coefficient of air-brush system, ρ_{Solution} is the density of solution, and ΔP is the pressure difference of the air-brush system. Eq.(1) is based on the equilibrium condition between Bernoulli pressure and surface tension. We will discuss this in detail in another article. It can be clearly observed that the morphology of the spots is not smooth but has narrow and thick edge around the thin bottom. This phenomenon can be explained by the coffee ring effect[14]. The air brushing film is accumulated by huge number of uneven spots in amorphous shape. Therefore, they often have quite rough surface. It can be proved by the surface profiles of both buffer and active layers as shown in Fig.4(a) and (b). Besides, the thicknesses of buffer and active layers can be observed from the "steps" on the left side of Fig.4(a) and (b), which are about 400 nm for buffer layer and about 600 nm for active layer. These are much thicker than those of spin coating device, because air brushing film needs enough spots, which can be observed in Fig.3(b), to form continuous film and avoid electric leakage caused by dusts from the atmosphere.

The rough surface of polymer film often leads to weak performance of PSCs. However, sometimes it is not serious. An interesting consequence is observed on the air brushing device. The *J-V* curves of devices are shown in Fig.5(a), the details are shown in Tab.2, and the IPCE spectra are shown in Fig.5(b). The open-circuit voltage (V_{oc}) and the fill factor (*FF*) of the air brushing devices are not satisfactory. It can be explained by high interface barrier and leakage between anode and cathode caused

by rough surface of film. However, high current density is obtained, and the conversation efficiency is also acceptable.

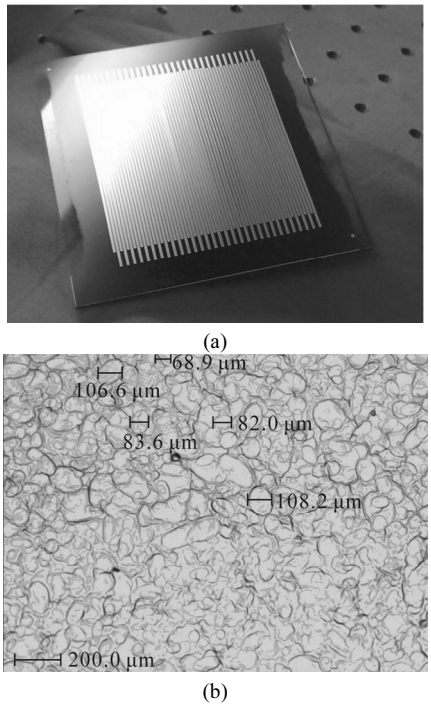

Fig.3 (a) Photo of the matrix device; (b) Microscopic photo of the matrix device without cathode

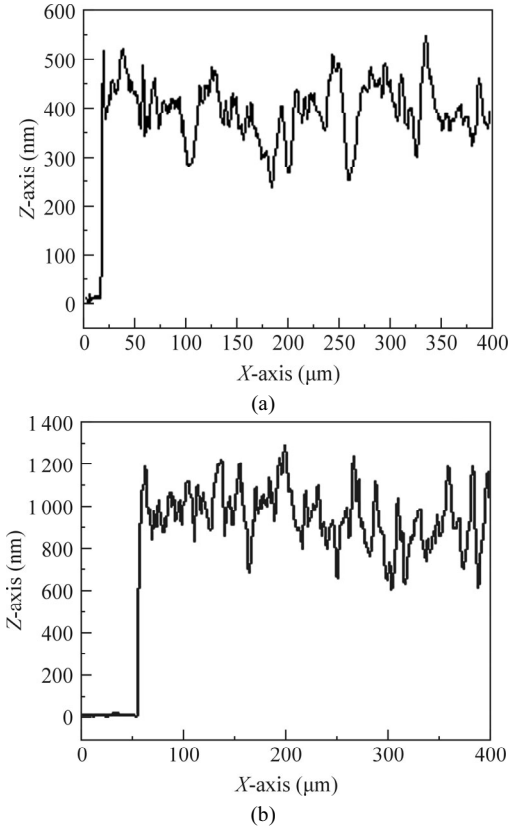

Fig.4 Surface profiles of (a) PEDOT:PSS buffer layer and (b) P3HT:PCBM active layer

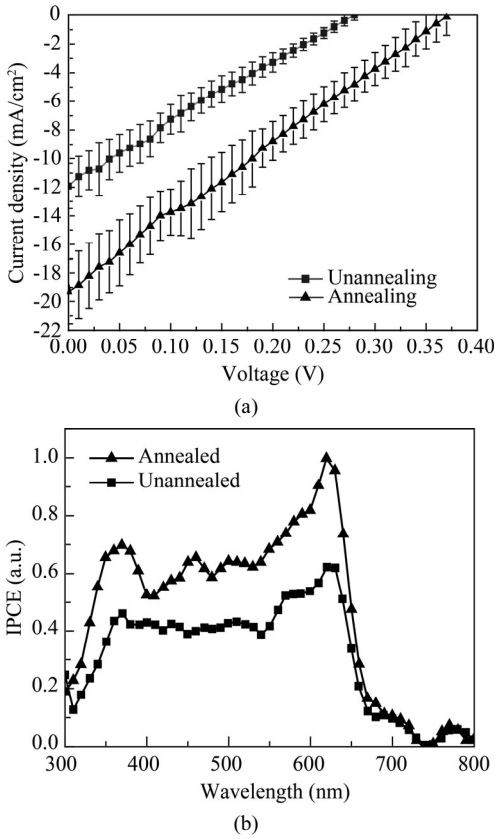

Fig.5 (a) *J-V* curves and (b) IPCE curves of small size PSCs on the matrix device with and without annealing

Tab.2 The parameters of small PSCs on the matrix device

Annealing	V_{oc} (V)	J_{sc} (mA)	*FF*	η (%)
Unannealed	0.280±0.013	11.91±1.58	0.244±0.022	0.815±0.136
Annealed	0.374±0.026	19.29±2.25	0.254±0.019	1.820±0.343

The reason can be found on the surface profiles shown in Fig.4. The buffer/active and active/cathode interfaces are both not flat as the idealized model shown in Fig.1(c). It is a finger joint structure as the schematic diagram shown in Fig.6. It is well known that the exciton dissociation efficiency is very high at bulk heterojunction active layer. However, the phase separation is usually not continuous. Massive donor or acceptor isolated islands exist in the active layer, and the transmission of photon-generated carriers on these islands is greatly constrained. In the finger joint structure, the interfacial areas of both buffer/active and active/cathode are significantly increased. Moreover, lots of highly conductive PEDOT:PSS and Al peaks stab into active layer and connect many isolated islands. Thus more photon-generated carriers can be collected by the electrode. As a result, the current density of device can be significantly enhanced.

It can be seen from the results that the annealing

process improves the performance of devices significantly, because it can improve the phase separation in both PEDOT:PSS and P3HT:PCBM layers and the interface contact by discharging residual gas brought in the process of spraying. By optimizing conditions, the conversion efficiency of annealed device reaches 1.820±0.343%, and the current density is obtained as 19.29±2.25 mA/cm^2.

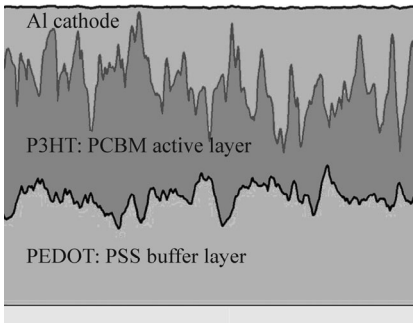

Fig.6 Schematic diagram of the real air-brush device

In summary, a 64 mm×64 mm matrix PSC is fabricated by air-brush spray deposition. Although V_{oc} and *FF* need to be improved, the conversion efficiency of the matrix PSC still reaches about 1.82%, and especially the current density nearly 20 mA/cm^2 is obtained. The results verify that air-brush spray deposition is a suitable method to prepare large area PSC device, and the process we use in this paper can be easily transplanted to roll-to-roll production. By optimizing preparation conditions, air-brush spray deposition will be one of the most promising methods which can be used in industrial production in the future.

References

[1] C. W. Tang, Applied Physics Letters **48**, 183 (1986).
[2] C. J. Brabec, N. S. Sariciftci and J. C. Hummelen, Advanced Functional Materials **11**, 15 (2001).
[3] WU Ming-xiao, TIAN Jin-peng, TU Cheng-wei, XIE Wei-guang and LIU Peng-yi, Journal of Optoelectronics·Laser **26**, 63 (2015). (in Chinese)
[4] SU Bin, ZHANG Xin-xin, LIU Chun-bo, CHE Guang-bo, DU Wen-qiang, HAO Meng, LIU Shu-yu and XU Chun-hui, Journal of Optoelectronics·Laser **25**, 2279 (2014). (in Chinese)
[5] WANG Fu-zhi, SUN Gang and TAN Zhan-ao, Journal of Optoelectronics·Laser **25**, 658 (2014). (in Chinese)
[6] C. J. Brabec, Solar Energy Materials and Solar Cells **83**, 273 (2004).
[7] L. L. Kazmerski, Best Research-Cell Efficiencies, National Renewable Energy Laboratory (NREL), Dec. 5th, 2011.
[8] F. C. Krebs, Solar Energy Materials and Solar Cells **93**, 394 (2009).
[9] C. N. Hoth, S. A. Choulis, P. Schilinsky and C. J. Brabec, Advanced Materials **19**, 3973 (2007).
[10] T. Aernouts, T. Aleksandrov, C. Girotto, J. Genoe and J. Poortmans, Applied Physics Letters **92**, 033306 (2008).
[11] F. C. Krebs, M. Jørgensen, K. Norrman, O. Hagemann, J. Alstrup, T. D. Nielsen, J. Fyenbo, K. Larsen and J. Kristensen, Solar Energy Materials and Solar Cells **93**, 422 (2009).
[12] D. J. Vak, S. S. Kim, J. Jo, S. H. Oh, S. I. Na, J. H. Kim and D. Y. Kim, Applied Physics Letters **91**, 081102 (2007).
[13] R. Green, A. Morfa, A. J. Ferguson, N. Kopidakis, G. Rumbles and S. E. Shaheen, Applied Physics Letters **92**, 033301 (2008).
[14] R. D. Deegan, O. Bakajin, T. F. Dupont, G. Huber, S. R. Nagel and T. A. Witten, Nature **389**, 827 (1997).